

The Phase Transition to a Square Vortex Lattice in Type-II Superconductors with Fourfold Anisotropy

Kyungwha Park and David A. Huse

Department of Physics, Princeton University, Princeton, NJ 08544

March 24, 2022

Abstract

We investigate the stability of the square vortex lattice which has been recently observed in experiments on the borocarbide family of superconductors. Taking into account the tetragonal symmetry of these systems, we add fourfold symmetric fourth-derivative terms to the Ginzburg-Landau(GL) free energy. At H_{c2} these terms may be treated perturbatively to lowest order to locate the transition from a distorted hexagonal to a square vortex lattice. We also solve for this phase boundary numerically in the strongly type-II limit, finding large corrections to the lowest-order perturbative results. We calculate the relative fourfold H_{c2} anisotropy for field in the xy plane to be 4.5% at the temperature, T_c^\square , where the transition occurs at H_{c2} for field along the z axis. This is to be compared to the 3.6% obtained in the perturbative calculation. Furthermore, we find that the phase boundary in the $H - T$ phase diagram has positive slope near H_{c2} .

1 Introduction

The possibility of square vortex lattices in type-II superconductors was first proposed by Abrikosov [1] in his original paper on vortex lattices. However, it

was later shown that the hexagonal vortex lattice has a lower free energy for isotropic materials. [2] Anisotropy in the effective mass or superfluid density tensors cause distortions of this hexagonal lattice simply in proportion to the anisotropy of the magnetic penetration length. Effects due to higher-order anisotropies (e.g., in cubic crystals) were seen in the 1970's for some low κ superconductors such as PbTl, PbBi, and Nb. [3] In some cases, when the external magnetic field was applied along a fourfold symmetric axis of the crystal, the vortices formed a square lattice. When the field was applied along the threefold or twofold symmetric axis of the crystals, hexagonal or distorted hexagonal lattices were observed, respectively. In the case of Nb, for field along [001] the square vortex lattice transformed into a hexagonal lattice as the temperature or field increased. Takanaka [4] introduced terms with cubic anisotropy into the phenomenological Ginzburg-Landau(GL) theory to explain the vortex lattice structures quite successfully. The extra terms arise from anisotropy of the Fermi surface.

Recently, in $\text{ErNi}_2\text{B}_2\text{C}$, one of the borocarbide family of superconductors, Yaron, *et al.*[5] and Eskildsen, *et al.*[6] have used neutron scattering and Bitter decoration to observe the phase transition from a distorted hexagonal vortex lattice aligned with either the [100] or [010] directions to a square vortex lattice aligned with the [110] direction for increasing magnetic field along the [001] direction. This was the first observation of a square vortex lattice in a strongly type-II material with $\kappa \gg 1/\sqrt{2}$. These experiments have motivated further theoretical and experimental studies. Kogan *et al.* [7] have analyzed the vortex lattice transition in borocarbides by taking into account the fourfold anisotropic corrections to the London model in the intermediate field region and $T \ll T_c$. This study revealed two kinds of phase transitions: at small fields (along the [001] direction), the distorted hexagonal lattice is aligned with a [110] direction. As the field increases, the lattice reorients along a [100] direction in a first-order phase transition. At a still higher field the square vortex lattice becomes stable. The latter phase transition is continuous. The square vortex lattice has also been observed in other borocarbides such as $\text{LuNi}_2\text{B}_2\text{C}$ [9] and $\text{YNi}_2\text{B}_2\text{C}$ [10], using scanning tunnelling microscopy (STM) and neutron scattering, respectively.

Vortex lattice structures in the high-temperature superconductors have also been studied. For low applied fields along the c axis (normal to the copper-oxide planes), the flux lattice can be seen using Bitter decoration. A distorted hexagonal lattice was seen for YBCO, [11] distorted as expected

from the in-plane (ab) effective mass anisotropy. But the STM pictures of the vortex lattice obtained at much higher field [12] are more consistent with a square lattice that is distorted by effective mass anisotropy. Thus it appears that the hexagonal to square lattice transition that we are studying may also occur in YBCO. Motivated by this, Affleck *et al.* [8] showed how fourfold anisotropic terms can arise in the London free energy due to a d -wave symmetry of the superconducting order parameter.

In this paper, we examine the structure of the vortex lattice near H_{c2} within a generalized Ginzburg-Landau (GL) free energy functional. We consider systems with tetragonal symmetry such as the borocarbides. The lowest-order term (ignoring effective mass anisotropy) that reduces the symmetry from isotropic down to tetragonal is fourth-order in the spatial derivative and second-order in the order parameter. We discuss the three distinct terms that can be added to the GL free energy at this order. These new terms may be treated perturbatively near H_{c2} to first order, demonstrating that the square lattice occurs at high fields where the higher-order gradient terms are more important, while the lattice distorts toward hexagonal at lower fields, in qualitative agreement with experiment. The phase transition, which we treat only on a mean-field level, is an Ising-type critical point, with the square unit cell distorting into a rhombus in two possible ways by increasing the length of one of its diagonals and reducing the other. The perturbation expansion has not been carried to higher order, so the quantitative accuracy of the first-order approximation had not previously been estimated. To investigate this we have numerically determined the phase diagram of this system, locating the upper critical field for various field orientations and the phase boundary separating the square and distorted hexagonal vortex lattice phases. We find that there are substantial (up to 50%) differences from the perturbative approximation, for example in the location of the phase boundary. Thus although the first-order perturbative approximation gives a good qualitative description of the phase diagram, quantitatively accurate results require a proper treatment of higher-order effects.

2 Ginzburg-Landau model

To study the lowest free energy pattern of the vortex lattice near H_{c2} for tetragonal crystals, we use the Ginzburg-Landau (GL) theory with added

fourfold symmetric fourth-order derivative terms. The full free energy functional that we minimize (ignoring thermal fluctuations) is

$$F = F_0 + F_4. \quad (1)$$

F_0 is the usual GL free energy:

$$F_0 = \int d^3r \left\{ \alpha |\psi|^2 + \frac{\beta}{2} |\psi|^4 + \frac{1}{2m^*} |\vec{\Pi}\psi|^2 + \frac{\hbar^2}{8\pi} \right\}. \quad (2)$$

For simplicity, we have taken an isotropic effective mass tensor. Tetragonal symmetry, of course, also allows uniaxial effective mass anisotropy, but this can be scaled out by rescaling the z axis and the xy components of the magnetic field. The only resulting difference is then in the \hbar^2 field energy term in F_0 , but this does not affect any of our results below. F_4 contains the additional terms allowed with tetragonal symmetry that are of fourth order in the x and y gauge-invariant derivatives and second order in the order parameter:

$$\begin{aligned} F_4 = \int d^3r \frac{1}{4m^{*2}|\alpha|} & [\epsilon_i \tau |(\Pi_x^2 + \Pi_y^2)\psi|^2 \\ & + \epsilon_a \tau (|(\Pi_x^2 - \Pi_y^2)\psi|^2 - |(\Pi_x \Pi_y + \Pi_y \Pi_x)\psi|^2) \\ & + \frac{\epsilon_b \tau \hbar^2 e^{*2}}{c^2} h_z^2 |\psi|^2]. \end{aligned} \quad (3)$$

The gauge-invariant derivative is

$$\vec{\Pi} = \frac{\hbar}{i} \vec{\nabla} - \frac{e^*}{c} \vec{A}. \quad (4)$$

We are interested in $T < T_c$, so α is negative. τ is defined to be $1 - \frac{T}{T_c}$, so it is positive. $\vec{h}(\vec{r})$ is the local magnetic field, $\vec{h} = \vec{\nabla} \times \vec{A}$. F_4 contains two isotropic terms with coefficients ϵ_i and ϵ_b , and the anisotropic term with coefficient ϵ_a . The approximation of limiting the free energy to include only terms that are low-order in the gradient and the order parameter is valid for temperatures near T_c . Only terms that are of fourth or higher order in the x and y gradients can reduce the rotational symmetry about the z -axis from circular down to tetragonal, which is why we add the fourth-order terms to the usual GL free energy. The anisotropic term may arise simply from fermi-surface anisotropy [4] or from a d-wave nature of the pairing [8].

In the literature [8, 9], certain particular combinations of the isotropic and the anisotropic fourth order derivative terms in F_4 have been used. In our numerics (below), we will also use a specific convenient combination of them. For the theory as specified above to be stable, the fourth-derivative terms have to be non-negative, which requires $\epsilon_i \geq |\epsilon_a|$. In our notation, a term $\epsilon\tau(|\Pi_x^2 - \Pi_y^2|\psi|^2$ [8] corresponds to

$$\epsilon_i, \epsilon_a, \epsilon_b = \frac{\epsilon}{2}, \frac{\epsilon}{2}, \frac{3\epsilon}{2}. \quad (5)$$

A term $\epsilon\tau(|\Pi_x^2\psi|^2 + |\Pi_y^2\psi|^2)$ [9] corresponds to

$$\epsilon_i, \epsilon_a, \epsilon_b = \frac{3\epsilon}{4}, \frac{\epsilon}{4}, \frac{3\epsilon}{4}. \quad (6)$$

And the term $\epsilon\tau(|\Pi_x\Pi_y + \Pi_y\Pi_x|\psi|^2$ that we use in our numerics corresponds to

$$\epsilon_i, \epsilon_a, \epsilon_b = \frac{\epsilon}{2}, -\frac{\epsilon}{2}, \frac{3\epsilon}{2}. \quad (7)$$

In F_4 , the anisotropic term is the one that causes the vortex lattice to distort and become square when the field is along the z axis and $|\epsilon_a|\tau$ is large enough. The isotropic terms do not by themselves cause any distortion of the hexagonal vortex lattice, but they do change H_{c2} .

For convenience, we introduce the following ‘‘dimensionless’’ units: the magnetic field is measured in units of $H_{c2} = \phi_0/(2\pi\xi^2)$, the vector potential in units of $H_{c2}\xi$, the length in units of the coherence length $\xi = \hbar/\sqrt{2m^*|\alpha|}$, the order parameter in units of the zero-field order parameter magnitude: $|\psi_\infty| = \sqrt{|\alpha|/\beta}$, and the energy in units of $H_c^2\xi^3/4\pi$. Using these units, the free energy (1) is

$$\begin{aligned} F = \int d^3r [& -|\psi|^2 + \frac{1}{2}|\psi|^4 + |\vec{\Pi}\psi|^2 + \kappa^2 h^2 + \epsilon_i\tau(|\Pi_x^2 + \Pi_y^2|\psi|^2 \\ & + \epsilon_a\tau(|\Pi_x^2 - \Pi_y^2|\psi|^2 - |(\Pi_x\Pi_y + \Pi_y\Pi_x)\psi|^2) \\ & + \epsilon_b\tau h_z^2|\psi|^2], \end{aligned} \quad (8)$$

with

$$\vec{\Pi} = \frac{\vec{\nabla}}{i} - \vec{A}. \quad (9)$$

3 Perturbative results

First we look at the vortex lattice behavior at H_{c2} by treating F_4 as a perturbation to the usual GL theory, F_0 , obtaining the free energy to first order in F_4 . Most of these results were first presented by Takanaka [4], and then, much more recently, by De Wilde, *et al.* [9].

Because of F_4 , the upper critical field depends on the field orientation. When the field is along the z axis, the upper critical field (in the absence of fluctuations) is given by

$$H_{c2}[001] = \frac{\phi_0}{2\pi\xi^2}(1 - \epsilon_i\tau - \epsilon_b\tau + \dots). \quad (10)$$

When the field is in the xy plane,

$$H_{c2}[xy0] = \frac{\phi_0}{2\pi\xi^2}\left(1 - \frac{3}{4}(\epsilon_i\tau + \epsilon_a\tau \cos 4\phi) + \dots\right), \quad (11)$$

where ϕ is the angle between the field and the x axis. The relative xy -plane anisotropy of the upper critical field is thus

$$\Delta H_{c2}/H_{c2} = (H_{c2}[100] - H_{c2}[110])/H_{c2}[100] \quad (12)$$

$$= -\frac{3\epsilon_a\tau}{2} + \dots \quad (13)$$

Near H_{c2} the GL free energy density, including the first-order perturbative contributions from F_4 , may be simplified by the Abrikosov identities[1, 4, 13]. For the field along the z axis, this gives

$$f = \kappa^2 \left[B^2 - \frac{(B - H_{c2}(\epsilon_i\tau, \epsilon_b\tau))^2}{1 - \frac{\langle h_s^2 \rangle}{\langle h_s \rangle^2} + \frac{\langle |\psi_L|^4 \rangle}{2\kappa^2 \langle h_s \rangle^2}} \right], \quad (14)$$

where ψ_L is the solution of the linearized GL equation at H_{c2} , including the terms from F_4 . h_s is defined by $h = H + h_s$, where H is the applied field; all fields are along the z axis. $\langle \dots \rangle$ means a spatial average over the vortex lattice, and $B = \langle h \rangle$ is the spatial average of the magnetic field. The free energy density (14) can be written in terms of the Abrikosov ratio β_A as

$$f = \kappa^2 \left[B^2 - \frac{(B - H_{c2}(\epsilon_i\tau, \epsilon_b\tau))^2}{1 + (2\kappa^2 - 1)\gamma\beta_A(\epsilon_a\tau)} \right], \quad (15)$$

$$\gamma \equiv 1 - \frac{8\kappa^2(\epsilon_i\tau + \epsilon_b\tau) - \frac{2\epsilon_b\tau}{3}}{2\kappa^2 - 1},$$

where

$$\begin{aligned}\beta_A &\equiv \frac{\langle |\psi_L|^4 \rangle}{\langle |\psi_L|^2 \rangle^2} \\ &= \beta_0 - \epsilon_a \tau Re\beta_4,\end{aligned}\tag{16}$$

$$\beta_{2n} = \frac{\langle (\Pi_+^{2n} \psi_0) \psi_0^* |\psi_0|^2 \rangle}{\langle |\psi_0|^2 \rangle^2 2^n}.\tag{17}$$

ψ_0 is the solution to the linearized GL equations when $\epsilon_{i,a,b} = 0$, and Π_+ is $\Pi_x - i\Pi_y$. We obtain the stable pattern of the vortex lattice just below H_{c2} by minimizing the Abrikosov ratio, β_A . For regular vortex lattices with one vortex per unit cell, the lattice vectors are specified by (see Fig. 1)

$$\begin{aligned}\vec{a}_1 &= \left(\frac{L_x}{2}, -\frac{L_y}{2}\right), \\ \vec{a}_2 &= \left(\frac{L_x}{2}, \frac{L_y}{2}\right).\end{aligned}$$

(The vortex lattice may also be rotated from this orientation by angle $\pi/4$; this is equivalent to changing the sign of ϵ_a .) β_0 and β_4 can be written explicitly using the reciprocal lattice vectors as

$$\beta_0 = \sum_{p,q} \exp\left[-\frac{\pi}{2b}\{(p^2 + q^2)(1 + b^2) + 2pq(1 - b^2)\}\right],\tag{18}$$

$$\begin{aligned}\beta_4 &= \sum_{p,q} \frac{\pi^2}{4b^2} (p + q + i(-p + q)b)^4 \\ &\quad \exp\left[-\frac{\pi}{2b}\{(p^2 + q^2)(1 + b^2) + 2pq(1 - b^2)\}\right],\end{aligned}\tag{19}$$

where $b = L_x/L_y$. The sums run over all (positive, zero and negative) integer pairs. The square vortex lattice is $b = 1$ and the hexagonal lattice is $b = \sqrt{3}$ or $b = 1/\sqrt{3}$; other values of b we call distorted hexagonal lattices.

For small positive $|\epsilon_a|\tau$ the lowest free energy states for this system are distorted hexagonal lattices, and the square vortex lattices are local maxima of the free energy. To calculate the stability of the square lattice the second derivatives at $b = 1$ are needed: they are $d^2\beta_0/db^2 \cong -0.295$ and $d^2Re\beta_4/db^2 \cong 12.4$. Thus, within the approximation of calculating β_A to

only first order in ϵ_a , at H_{c2} the appropriately-oriented square vortex lattice changes from a local maximum of the free energy to a global minimum at

$$|\epsilon_a|\tau_c^\square \cong 0.0238. \quad (20)$$

For larger values of $|\epsilon_a|\tau$ the lowest free energy state of the vortex lattice is square. This critical value of $|\epsilon_a|\tau$ does not depend on κ at first order in ϵ_a . This first-order approximation then says that the phase transition from distorted hexagonal to square vortex lattice at H_{c2} for the field along the z axis is at the temperature where the xy -plane H_{c2} varies by about 3.6% from [100] to [110] field directions.

One way to get a sense of how accurate this first-order in F_4 approximation is would be to calculate the next corrections (second-order in F_4). This did not appear to be analytically tractable to us, so we have instead located the phase transition numerically, finding that there are indeed rather large corrections to this first-order approximation.

4 Numerical Study

At the order we are considering, in F_4 there are three different terms added to the usual Ginzburg-Landau theory, and F_0 contains κ and \vec{H} , which cannot be scaled away. In principle, one could examine the behavior in the full parameter space $(\vec{H}, \kappa, \epsilon_i, \epsilon_a, \epsilon_b)$. However, we are interested in the phase transition to the square vortex lattice that is caused by the anisotropic term, ϵ_a . If we add only this term, it can be negative so the free energy then becomes unbounded below and the system is unstable at short wavelengths. To stabilize the system we set $\epsilon_i = |\epsilon_a|$. We also set ϵ_b to keep H_{c2} at its original value of $\phi_0/(2\pi\xi^2)$ for field along the z axis. For simplicity, we will only examine the large κ limit, where the magnetic field is uniform. With all these constraints and simplifications, the system we studied numerically is, in dimensionless form:

$$F = \int d^3r \left[-|\psi|^2 + \frac{1}{2}|\psi|^4 + |\vec{\Pi}\psi|^2 + \epsilon\tau |(\Pi_x\Pi_y + \Pi_y\Pi_x)\psi|^2 + \epsilon_b\tau H_z^2 |\psi|^2 \right], \quad (21)$$

with $\epsilon\tau = 2\epsilon_i\tau = -2\epsilon_a\tau \geq 0$ and for each value of $\epsilon\tau$, $\epsilon_b\tau$ is chosen so that along the z axis $H_{c2} = 1$ in these units. In the first-order approximation

above, for field along the z axis the phase transition to the square vortex lattice at H_{c2} occurs at $\epsilon\tau \cong 0.048$. We find the higher-order corrections are substantial, and the actual transition in this system (21) does not occur until $\epsilon\tau_c^\square \cong 0.073$. Presumably the precise result for $\epsilon_a\tau_c^\square$ will vary, depending on the values of κ, ϵ_i and ϵ_b as well as other higher-order terms, all of which potentially differ between materials; we have not explored this dependence. Our basic message here is that the first-order in ϵ_a perturbative estimate is substantially off, so higher-order effects have to be treated properly to quantitatively estimate the phase diagram for any particular system.

The stable vortex lattice for this system (21) with the field along the z axis is shown in Fig. 1. The area of the unit cell is dictated by the magnetic field because there is exactly one flux quantum per vortex. The only remaining freedom is the angle, θ , between the two nearest-neighbor vectors shown in Fig. 1. The square lattice is $\theta = \frac{\pi}{2}$, the hexagonal lattice is $\theta = \frac{\pi}{3}$ (or $\frac{2\pi}{3}$); other angles are the distorted hexagonal lattices. The minimum free energy vortex lattice for each θ is an order parameter and current pattern that is symmetric under the operations that reverse the currents and then reflect in a plane that contains vortex lines and is parallel to the x or y axis. These symmetries mean we only have to determine the pattern over one quarter of the unit cell of the vortex lattice. We have chosen the quarter in the positive x and y quadrant (see Fig. 1).

We discretize the system on a rectangular numerical grid aligned with the x and y axes. We use gauge-invariant variables only, namely the magnitude $|\psi|$ of the order parameter at each grid point, and the gauge-invariant phase differences between nearest neighbor grid points along the x direction, $\Delta_x\phi$, and along the y direction, $\Delta_y\phi$. These phase differences are not all independent, since their sum around an elementary plaquette of the grid must be equal to Hd_xd_y , where d_x and d_y are the grid spacings. We put one grid point at the precise core of the vortex at the origin in Fig. 1; at this point $|\psi| = 0$ so the phase is ill-defined and special care must be taken when treating the terms involving this point.

All terms in the discretized GL free energy are symmetric so that the differences between the discretized expression and the continuum limit are even polynomials of d_x and d_y . We extrapolate to the continuum limit by reducing d_x and d_y together, keeping their ratio constant. Under these conditions the discretization errors are proportional to d_xd_y , the area of the grid

plaquette, for small d_x and d_y . For example, under our discretization

$$\begin{aligned} & \left| \left(\frac{\nabla_x}{i} - A_x \right) \psi(x, y) \right|^2 \rightarrow \\ & \frac{1}{d_x^2} \left| \left[\left| \psi \left(x + \frac{d_x}{2}, y \right) \right| \exp \left(\frac{i \Delta_x \phi}{2} \right) - \left| \psi \left(x - \frac{d_x}{2}, y \right) \right| \exp \left(-\frac{i \Delta_x \phi}{2} \right) \right] \right|^2. \end{aligned} \quad (22)$$

The boundary conditions on our quarter unit cell are

$$|\psi(0, 0)| = 0, \quad (23)$$

$$\left| \psi \left(x, \frac{L_y}{4} \right) \right| = \left| \psi \left(\frac{L_x}{2} - x, \frac{L_y}{4} \right) \right|, \quad (24)$$

$$\Delta_x \phi(x, 0) = 0, \quad (25)$$

$$\Delta_y \phi(0, y) = 0, \quad (26)$$

$$\Delta_y \phi \left(\frac{L_x}{2}, y \right) = 0, \quad (27)$$

$$\Delta_x \phi \left(x, \frac{L_y}{4} \right) = -\Delta_x \phi \left(\frac{L_x}{2} - x, \frac{L_y}{4} \right), \quad (28)$$

$$\Delta_y \phi \left(x, \frac{L_y}{4} \right) = -\Delta_y \phi \left(\frac{L_x}{2} - x, \frac{L_y}{4} \right); \quad (29)$$

we put grid points along all these boundaries.

We begin with smooth initial conditions that satisfy all of the above constraints. Then we minimize the discretized version of the GL free energy (21) using the relaxation method [14]

$$\psi^{new} = \psi^{old} - \Gamma \frac{\partial F}{\partial \psi^*} \Big|_{old}, \quad (30)$$

where Γ is a relaxation parameter which can be adjusted to avoid numerical instabilities and to hasten the convergence to the minimum.

We have obtained the minimum of the discretized free energy for grid sizes (12×6) , (16×8) , (20×10) , (24×12) , (28×14) , and (32×16) points for the square ($\theta = 90^\circ$) and two weakly distorted vortex lattices ($\theta = 88^\circ, 86^\circ$). For each H and $\epsilon\tau$ the dependence of the free energy on θ is extrapolated to the continuum limit. At H_{c2} we also obtain the Abrikosov ratio $\beta_A(\epsilon\tau, \theta)$. The critical parameter value above which the minimum Abrikosov ratio is at the square lattice ($\theta = 90^\circ$) is $\epsilon\tau_c^\square \cong 0.0734$. To determine the phase boundary below H_{c2} , we fix $\epsilon\tau$ and sweep the magnetic field to find the transition

Table 1: Transition fields, H^\square , for a few $\epsilon\tau$ values.

$\epsilon\tau$	H^\square/H_{c2}
0.0734	1.000
0.0800	0.901 ± 0.002
0.0860	0.826 ± 0.001
0.0930	0.752 ± 0.001
0.1000	0.687 ± 0.001

field, H^\square , above which the square vortex lattice is stable. Table 1 shows the transition fields for a few $\epsilon\tau$ values. Within our model, we certainly could follow the phase boundary to lower fields and temperatures, deeper into the vortex lattice phase. But the model, in the usual approach of Landau theory, has kept only certain terms that are low-order in an expansion in the order parameter, the gradients, and τ . The neglected higher-order terms become more important as one moves away from T_c to lower temperature and away from H_{c2} to lower fields. Thus the phase diagrams of real systems with different higher-order terms will increasingly diverge from the behavior we find in this specific model (21) as one goes to lower temperature. This is why we did not bother to follow the phase boundary to lower temperature than shown in Table 1.

The physically meaningful phase diagram in the magnetic field, temperature plane is shown in Figure 2, with the field and temperature axes scaled by the values of H and τ at the point $(H_c^\square, \tau_c^\square)$ where the phase boundaries $H^\square(T)$ and $H_{c2}(T)$ meet. Although the point at which this happens is at roughly 50% larger $\epsilon\tau$ than the estimate from the perturbative results, our phase diagram when scaled this way is very close to the one obtained perturbatively by De Wilde, *et al.*, [9] with the distorted hexagonal/square phase boundary meeting the upper critical field with a positive slope in the H, T plane (with this scaling, the slope of $H^\square(T)$ is about 0.2, while the slope of $H_{c2}(T)$ is -1.)

Since, for field along the z axis, the critical $\epsilon\tau_c^\square$ at H_{c2} obtained numerically is quite different from the perturbative estimate, we have also numerically calculated for this system (21) the relative anisotropy of H_{c2} in the x - y

plane at $\epsilon\tau_c^\square$. We find that the dependence of H_{c2} on the angle ϕ between the field and the x axis contains substantial harmonic content beyond the basic $\cos(4\phi)$ term that is present in the first-order estimate, again indicating contributions beyond first-order in ϵ . At $\epsilon\tau = \epsilon\tau_c^\square$, the in-plane H_{c2} variation from [100] to [110] directions is $\Delta H_{c2}/H_{c2} \cong 4.5\%$, which is again larger than the 3.6% estimated perturbatively. The in-plane anisotropy of $H_{c2}(\phi)$ has recently been measured for $\text{LuNi}_2\text{B}_2\text{C}$, where it grows to near 10% at low temperature, indicating that the transition to the square lattice does meet the upper critical field for this material.[15]

5 Conclusion

We have numerically determined the vortex lattice phase diagram for a generalized Ginzburg-Landau model (21) that includes higher-order terms that reduce the rotational symmetry to tetragonal. Although the results are qualitatively unchanged from the estimates obtained by treating the anisotropic term perturbatively to only first order, there are substantial quantitative differences. In particular, we find that for field along the z axis, the phase boundary in the field-temperature plane separating the distorted hexagonal and square vortex lattices meets the upper critical field line with a positive slope at a temperature T_c^\square . If the field is instead put in the xy plane at this same temperature, the difference in H_{c2} between the [100] and [110] directions is about 4.5%. Although this number must be a better estimate than the 3.6% obtained perturbatively, the full Ginzburg-Landau theory for any given material will contain other higher-order terms that may also have a small influence on this critical anisotropy value. Thus the precise value may vary somewhat away from our estimate.

References

- [1] A. A. Abrikosov, Soviet Physics JETP **5**, 1174 (1957).
- [2] W. H. Kleiner, L. M. Roth and S. H. Autler, Phys. Rev. **133**, 1226 (1964).

- [3] J. Schelten, R-4 in *Anisotropic Effects in Superconductors*, ed. by H. Weber (Plenum, New York, 1977).
- [4] K. Takanaka, Prog. Theor. Phys. **46**, 1301 (1971); R-3 in *Anisotropic Effects in Superconductors*, ed. by H. Weber (Plenum, New York, 1977).
- [5] U. Yaron *et al.*, Nature **382**, 236 (1996).
- [6] M. R. Eskildsen *et al.*, Phys. Rev. Lett. **78**, 1968 (1997).
- [7] V. G. Kogan *et al.*, Phys. Rev. B **54**, 12386 (1996); Phys. Rev. B **55**, R8693 (1997).
- [8] I. Affleck, M. Franz and M. H. S. Amin, Phys. Rev. B **55**, R704 (1997).
- [9] Y. De Wilde *et al.*, Phys. Rev. Lett. **78**, 4273 (1997).
- [10] M. Yethiraj *et al.*, Phys. Rev. Lett. **78**, 4849 (1997).
- [11] G. J. Dolan, *et al.*, Phys. Rev. Lett. **62**, 2184 (1989).
- [12] I. Maggio-Aprile, *et al.*, Phys. Rev. Lett. **75**, 2754 (1995).
- [13] *Superconductivity*, ed. by R. D. Parks (Marcel-Dekker, New York, 1969).
- [14] S. Adler and T. Piran, Rev. Mod. Phys. **56**, 1 (1984).
- [15] V. Metlushko *et al.*, Phys. Rev. Lett. **79**, 1738 (1997).

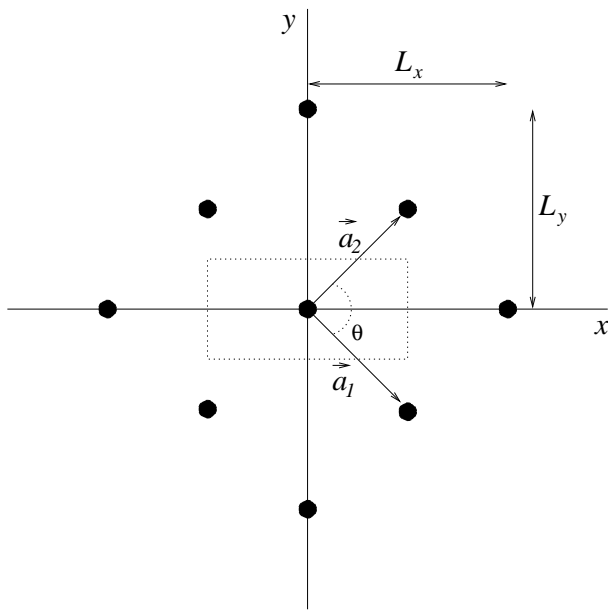


Figure 1: Geometry of the vortex lattice. The unit cell is drawn by the dotted line. The black dots represent vortices. \vec{a}_1, \vec{a}_2 are the lattice vectors.

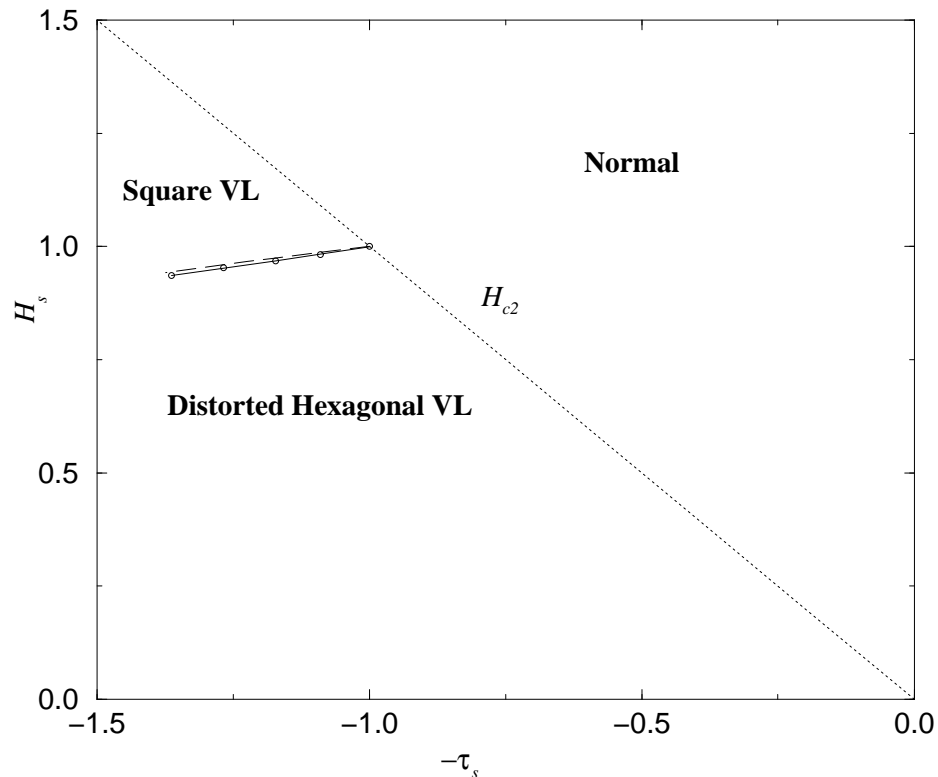


Figure 2: Phase diagram of our generalized Ginzburg-Landau model (21), scaled to the multicritical points $(T_c, H = 0)$ and $(T_c^\square, H_c^\square)$. The horizontal axis is the scaled $T - T_c$: $-\tau_s = -\tau/\tau_c^\square$, and the vertical axis is the scaled field: $H_s = H/H_c^\square$. The open circles represent our data points fitted to a polynomial function (solid line). For comparison, De Wilde,*et al.*'s result, scaled the same way, is drawn by the dashed line.